

Morphological and structural damage investigation of nanostructured molybdenum fuzzy surface after pulsed plasma bombardment

Yu-Chuan Luo(罗玉川), Rong Yan(鄢容), Guo Pu(蒲国), Hong-Bin Wang(王宏彬), Zhi-Jun Wang(王志君), Chi Yang(杨驰), Li Yang(杨黎), Heng-Xin Guo(郭恒鑫), Zhi-Bing Zhou(周志兵), Bo Chen(陈波), Jian-Jun Chen(陈建军), Fu-Jun Gou(苟富均), Zong-Biao Ye(叶宗标), and Kun Zhang(张坤)

Citation: Chin. Phys. B, 2022, 31 (**4**): 045203. DOI: 10.1088/1674-1056/ac3395
Journal homepage: http://cpb.iphy.ac.cn; http://iopscience.iop.org/cpb

What follows is a list of articles you may be interested in

Numerical simulation of anode heat transfer of nitrogen arc utilizing two-temperature chemical non-equilibrium model

Chong Niu(牛冲), Surong Sun(孙素蓉), Jianghong Sun(孙江宏), and Haixing Wang(王海兴)
Chin. Phys. B, 2021, 30 (**9**): 095206. DOI: 10.1088/1674-1056/ac133a

Decomposition reaction of phosphate rock under the action of microwave plasma

Hui Zheng(郑慧), Meng Yang(杨猛), Cheng-Fa Jiang(江成发), and Dai-Jun Liu(刘代俊)
Chin. Phys. B, 2021, 30 (**4**): 045201. DOI: 10.1088/1674-1056/abccb6

Estimation of tungsten production from the upper divertor in EAST during edge localized modes

Jing Ou(欧靖), Nong Xiang(项农), Zong-Zheng Men(门宗政), Ling Zhang(张凌), Ji-Chan Xu(许吉禅), Wei Gao(高伟)
Chin. Phys. B, 2019, 28 (**12**): 125201. DOI: 10.1088/1674-1056/ab5279

Numerical study of influence of $J\times B$ force on melt layer under conditions relevant to ITER ELMs

Yan Huang(黄艳), Ji-Zhong Sun(孙继忠), Juan Cai(蔡娟), Zhen-Yue Sun(孙振月), Chao-Feng Sang(桑超峰), De-Zhen Wang(王德真)
Chin. Phys. B, 2019, 28 (**4**): 045201. DOI: 10.1088/1674-1056/28/4/045201

Radiative divertor behavior and physics in Ar seeded plasma on EAST

Jingbo Chen(陈竞博), Yanmin Duan(段艳敏), Zhongshi Yang(杨钟时), Liang Wang(王亮), Kai Wu(吴凯), Kedong Li(李克栋), Fang Ding(丁芳), Hongmin Mao(毛红敏), Jichan Xu(许吉禅), Wei Gao(高伟), Ling Zhang(张凌), Jinhua Wu(吴金华), Guang-Nan Luo(罗广南), EAST Team
Chin. Phys. B, 2017, 26 (**9**): 095205. DOI: 10.1088/1674-1056/26/9/095205

Morphological and structural damage investigation of nanostructured molybdenum fuzzy surface after pulsed plasma bombardment

Yu-Chuan Luo(罗玉川)[1], Rong Yan(鄢容)[2], Guo Pu(蒲国)[1], Hong-Bin Wang(王宏彬)[1], Zhi-Jun Wang(王志君)[3], Chi Yang(杨驰)[3], Li Yang(杨黎)[1], Heng-Xin Guo(郭恒鑫)[1], Zhi-Bing Zhou(周志兵)[1], Bo Chen(陈波)[1], Jian-Jun Chen(陈建军)[1], Fu-Jun Gou(苟富均)[1], Zong-Biao Ye(叶宗标)[1,†], and Kun Zhang(张坤)[1,‡]

[1] *Key Laboratory of Radiation Physics and Technology of the Ministry of Education, Institute of Nuclear Science and Technology, Sichuan University, Chengdu* 610064, *China*

[2] *Institute of Plasma Physics, Hefei Institutes of Physical Science, Chinese Academy of Sciences, Hefei* 230031, *China*

[3] *Institute for Advanced Study, Chengdu University*, 2025 *Chengluo Avenue, Chengdu* 610106, *China*

(Received 19 August 2021; revised manuscript received 19 October 2021; accepted manuscript online 27 October 2021)

Steady high-flux helium (He) plasma with energy ranging from 50 eV to 90 eV is used to fabricate a fiber-form nanostructure called fuzz on a polycrystalline molybdenum (Mo) surface. Enhanced hydrogen (H) pulsed plasma in a wide power density range of 12 MW/m^2–35 MW/m^2 is subsequently used to bombard the fuzzy Mo, thereby simulating the damage of edge localized mode (ELM) to fuzz. The comparisons of surface morphologies, crystalline structures, and optical reflectivity between the original Mo and the Mo treated with various He^+ energy and transient power densities are performed. With the increase of He ion energy, the Mo nano-fuzz evolved density is enlarged due to the decrease of filament diameter and optical reflectivity. The fuzz-enhanced He release should be the consequence of crystalline growth and the lattice shrinkage inside the Mo-irradiated layers ($\sim$ 200 nm). The fuzz induced by lower energy experiences more severe melting damage and dust release under the condition of the identical transient H plasma-bombardment. The H and He are less likely to be trapped due to aggravated melting evidenced by the enhanced crystalline size and distinct lattice shrinkage. As the transient power density rises, the thermal effect is enhanced, thereby causing the fuzz melting loss to aggravate and finally to completely disappear when the power density exceeds 21 MW/m^2. Irreversible grain expansion results in huge tensile stress, leading to the observable brittle cracking. The effects of transient thermal load and He ion energy play a crucial role in etching Mo fuzz during ELM transient events.

Keywords: molybdenum nanostructured fuzz, pulsed-H plasma, edge localized mode, etching process

PACS: 52.40.Hf, 52.55.Pi, 52.55.Rk **DOI:** 10.1088/1674-1056/ac3395

1. Introduction

The resistance of plasma-facing material (PFM) to high-flux ions and heat load is indispensable to the stable operation of nuclear fusion devices.[1] Compared with other high refractory metals, the proposed alternative molybdenum (Mo) exhibits prominent advantages in withstanding such an extreme radiation environment due to its lower sputtering yield, higher thermal conductivity, and specific heat of vaporization,[2] while maintaining high optical reflectivity[3] and reducing hydrogen isotope retention[4] after interaction with the high-flux particles. Thus considering such an excellent performance, crystalline Mo is regarded as one of the basic candidate plasma-facing materials for part of the first wall in the tokamak device.[5]

Recently, helium (He) plasma-induced nanostructures in fiber form, called fuzz, have been observed on high refractory metal surfaces such as W or Mo under various plasma conditions in tokamak and linear plasma devices.[6–14] The formation mechanism of the fuzz structure is attributed to the trapping of He by thermal vacancies in these materials. The holes and protrusions induced by near-surface He bubbles act as seeds for forming the finer nanostructures.[15] The filament is fragile and porous, for it contains swelling He bubbles that have been observed by transmission electron microscope (TEM) in previous studies,[16] so that it is easily detached from the metal surface. The detailed studies have been carried out to confirm the formation conditions of such structures under the condtion of a certain surface temperature and incident ion energy, revealing that the fuzz can easily develop on the metal surfaces as long as the operation condition is satisfied.[17,18]

More importantly, type-I edge-localized mode (ELM) is usually generated when the tokamak plasma operates in the H-mode.[19] Considerable energy flows together with high-density deuterium–tritium ion flows are deposited on the plasma-facing surface.[20] Nevertheless, the critical issue of whether the He-induced modification is detrimental to the

†Corresponding author. E-mail: zbye@scu.edu.cn
‡Corresponding author. E-mail: kzhang@scu.edu.cn

© 2022 Chinese Physical Society and IOP Publishing Ltd

plasma-facing surface remains controversial. On the one hand, it has been found that the W nanostructure can suppress the surface cracking and D retention during transient plasma exposure.[21] On the other hand, the lower mechanical and thermal strength of W nanostructure reduce the transient damage threshold.[22] The interactions of fuzzy surfaces with transient loads simulated by plasma gun and laser reveal that the arcing is more prone to occur on fuzzy surfaces during ELMs, leading the impurities and dust to release.[23]

As one of the candidate materials for plasma-facing first mirror materials, Mo is a kind of high Z material similar to W. Even a small amount of Mo fuzz injection can contaminate the confined plasma, causing the plasma to cool down and finally threatening the sustainability of controlled fusion.[24] Pulsed Nd:YAG millisecond laser has been used to simulate transient heat loading to study the deformation of this structure during ELMs, revealing that the mass loss of Mo fuzz nanostructure and the rate of emission increase with the energy density and pulse count increasing.[25] However, the research work on the interaction between Mo fuzzy surface and pulsed plasma load is still lacking. Thus it is necessary to investigate the erosion process of Mo fuzz facing the high-density transient plasma.

In this paper, to replicate the irradiation conditions of plasma-facing materials, Mo fuzz nanostructure induced by steady He plasma is bombarded by an H-stabilized high-current plasma beam. Compared with previous irradiation methods, its extreme loading condition combining high heat load and ion fluxes is even closer to ELMs in the fusion-plasma environment. Moreover, the irradiation conditions can be flexibly adjusted by using helium ion energy and transient heat load. The synergistic effects of He ion beam and H transient thermal load on the morphological and crystalline structural evolution of Mo fuzz during ELMs are systematically studied in the present experiment. This study emphasizes a better understanding of the damage of Mo nanostructured fuzz during transient events and a reference for sustaining the performance of Mo plasma-facing materials in future fusion devices.

2. Experimental details

The pristine Mo disks each with a diameter of 20 mm and thickness of 1.5 mm were used as samples in the irradiation experiment. Prior to He and H plasma exposures, the samples were mechanically polished into a mirror-finished surface. Then the polished samples were cleaned thrice in a turn by deionized water, ethanol, and acetone in sequence to remove the surface residues and finally dried in the blast oven.

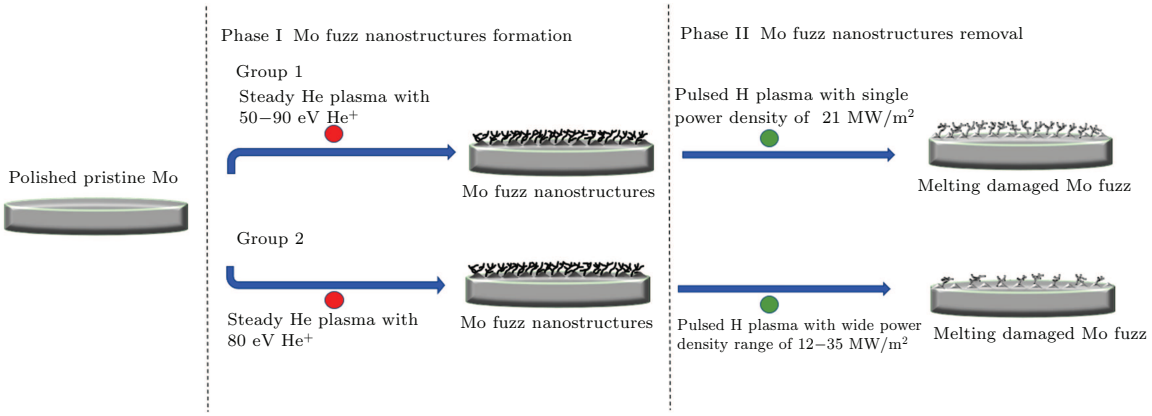


Fig. 1. Scheme of two-step strategy for plasma irradiation of Mo samples.

After the pretreatment process, the treated Mo samples would experience the irradiation process. As shown in Fig. 1, the treated pristine Mo samples were irradiated in two steps. In step 1, the Mo nano-fuzz structure was successfully synthesized by steady high-flux helium plasma with helium ion energy raging from 50 eV–90 eV. After being exposed to helium plasma, the Mo fuzzy samples were bombarded by enhanced H-pulsed plasma, thereby simulating the fuzz damage caused by transient events like ELMs. In step 2, the prepared fuzzy samples were divided into two groups. For group 1, taking into account the dispersion of helium ion energy interacting with the plasma-facing components (PFC) in a fusion device, Mo fuzz nanostructure induced by various He ion energy in a range of 50 eV–90 eV was irradiated by density-fixed H-pulsed plasma. For group 2, six Mo fuzzy surfaces prepared by identical He ion energy (80 eV) were respectively treated by pulsed-H plasma with higher or lower power density in a wider range. The power density of pulsed-H plasma (12 MW/m^2–35 MW/m^2) was adjusted by the discharge power, thereby simulating the aggravated serious ELM transient events. The designed two experimental groups aim to comprehensively investigate the influence of helium ion energy and transient thermal load on the erosion process of fuzz nanostructures after ELMs.

To achieve the experimental strategy discussed above, linear plasma devices have played an important role in simulating

operating conditions to study the interactions between high-heat-flux plasmas and surfaces. During being exposed to the He plasma exposure, steady high flux He plasma was generated by the linear plasma device based on a single cathode discharge as shown in supporting information0, Fig. S1.[26] The prepared samples were clamped on a molybdenum holder located on the plasma beam downstream at 40 cm. The thermocouple was placed beneath the irradiated molybdenum surface to timely monitor the temperature during the He plasma irradiating the sample, the temperature range for fuzz formation induced by different helium ion energies was 850 K–930 K, which was within the necessary temperature range of Mo surface fuzz nanostructure growth (800 K–1050 K). The discharge power of 10 kW, the gas flow of 5 standard liters per minute (SLM), and the axial magnetic field of 0.25 T were used to generate a magnetized cylindrical plasma beam. Steady He plasma irradiation was performed at a flux of 5.0×10^{22} ions·m^{-2}·s^{-1} and a total fluence of 1.2×10^{26} ions·m^{-2}. The energy of He ions was adjusted by the negative bias voltage applied to the molybdenum target, ranging from -50 V to -90 V. The energy of He^+ was chosen to replicate the working conditions of plasma-facing materials in future ITER with the steady He flux to the plasma-facing components being at energy in a range of 20 eV–100 eV. Besides, the necessary condition for growing the Mo fuzz structure in previous studies show that the incident He ion energy was in a range of 50 eV–100 eV. Therefore, the He^+ energy range for fuzz fabrication was determined to be within 50 eV–90 eV. Fuzz nanostructures at different ion energies could form on the pristine sample surface that is injected vertically by the steady-state He plasma flux.

The Mo fuzzy surface having been exposed to the steady-state He plasma, its response to transient loads is investigated by using a high-current plasma beam combining high-flux ions and heat loads.[27] The working gas was H_2 for the sake of simulating the escaped hydrogen particles interacting with PFM. The H ion density in a stabilized high-current plasma beam was enhanced in a three-circuit experiment designed in a compact linear device. The apparatus consisted of three pulsed discharge circuits, a vacuum chamber, and magnetic field coils, thereby allowing a high-density pulsed plasma to pass from the plasma generator to bombard the fuzzy molybdenum samples (see supporting information in Fig. S2). The plasma densities during the pulse were measured by using a single-channel CO_2 laser dispersion interferometer. The heat load density of pulsed plasma was determined by the voltage and current data detected by Rogowski coils. Note that the pulse width was around 1 ms and the heat flux could reach 35 MW/m^2 to replicate the condition of transient events in future tokamak devices. For choosing the transient power density, the transient power density was determined by the discharge voltage of discharge circuit. The experimental apparatus consisted of a large primary vacuum chamber to which a smaller chamber is attached for housing solid Mo target #2. The purpose of the configuration was to permit a high-current pulse to pass through the full length of the primary chamber. Power supplies #1 and #2 were set to be triggered simultaneously followed by power supply #3. We adjusted the supply voltage of power supply #3 in a wide range of 1000 V–2000 V, and the internal increase of voltage supply was 200 V. With the increase of voltage supply, the enhanced transient power densities were measured by internal voltage and current of the pulsed plasma beam. The rise of voltage supply in gradient aimed to closely simulate severe transient events growing in the fusion device. By comparing the extents of damage from various pulsed-plasma irradiations, the transient thermal load-dependant study can be carried out. Such studies have been recognized as increasingly important for the success of ITER and further fusion-energy development.

Several characterization methods were used to systematically track the evolution of the molybdenum surface after being irradiated by the plasma. For morphological studies, the topographical evolution of irradiated samples was visually observed by *ex-situ* field emission scanning electron microscopy (FE-SEM) and the optical profiler. To better quantitatively characterize the feature of irradiated surface, the root-means-square (RMS) roughness was also obtained by optical profiler graphs. Reflectivity measured by ultraviolet-visible spectrophotometer (UV-VIS) was an effective indicator of the fuzz nanostructure density. The wavelength of the light for the optical reflectivity measurement was in a range of 250 nm–850 nm, together with *ex-situ* mass loss measurement, enabling the qualitative analyzing of the density of fuzz due to the transient loading process. For crystal structure analysis, the grazing incident x-ray diffraction (GIXRD) measurements from 30° to 90° with an incident angle of 1° were used to analyze the crystal structure change of molybdenum surfaces before and after being irradiated. Our characterizations could provide a reference to a better understanding of the damage of edge plasma to plasma-facing materials during transient events.

3. Results and discussion

3.1. Preparation of Mo fiber-formed fuzz nanostructures

When the incident ion energy is below the threshold for atom displacement, strong morphology changes, such as blister formation have been observed recently, which is especially pronounced in the case of low-energy helium ions.[28] The molybdenum surfaces exposed to low energy (50 eV–100 eV) helium ions with large fluences are found to form nanostructure consisting of nanoscale filaments named fuzz.[18] Detailed studies have been conducted to explain the formation mechanism of such structures, which is related to the coalescence

of helium bubbles finally inducing swelling of the surface.[16] The variations of Mo nano-fuzz induced by different helium ion energy are systematically characterized in this section.

3.1.1. The surface morphological characterization for denser fiber-form fuzz

Significant morphology changes are observed on the surfaces of Mo samples due to nano-fuzz formation. The silvery surface gradually turned optically black because the optical reflectivity of the molybdenum surface can reduce significantly to almost 0% due to the presence of denser Mo fuzz. As shown in Fig. 2(a), the FE-SEM images of a pristine Mo sample each show a flat and clean surface with few scratches formed during mechanical polishing. After being irradiated by the high-flux He plasma with energy of 50 eV, the surfaces of samples are found to have a great many of pinholes together with protrusions. With the help of active surface diffusion, the large bubbles push up the surface, resulting in the formation of blisters. And the burst of blisters causes the protrusions to form. The nucleation and growth of helium bubbles will intersect with the metal surface, forming protrusions and pinholes when He ion energy is relatively low. The surface roughness including the holes and protrusions act as seeds for forming the finer nanostructures. A similar observed experimental phenomenon was also reported by Cipiti *et al.*[29] As illustrated in Fig. 2(c), since the implanted He atoms are difficult to dissolve in metals, substitutional and interstitial He atoms tend to be trapped by thermal vacancies and collide with each other.[30] Rapid diffusion and accumulation of He atoms lead He bubble to form in the near-surface region, which should be responsible for a large number of protrusions and holes on the rough surface. With the increase of helium ion energy, it can be observed from Fig. 2(a) that the surface is fully covered with thinner fiber-form filaments with the increase of density originating from the original pinholes and protrusions. More elongated and intertwined filaments are formed on the top of the thicker protrusions, and more filaments and filamentous attachments are stacked and adhered to cover and wrap the protrusions as shown in Figs. 2(c). To further compare the morphology of fuzz after being treated by He plasma with various energy, the three-dimensional (3D) appearances are measured by the optical profiler to investigate the development of the fuzz structure as shown in Fig. 2(b). The maximum altitude discrepancy with plasma energy is displayed in 3D images from the optical profiler, in which the fuzzy surface is much rougher than that of the pristine surface and the roughness degree is accelerated by the enhancement of He plasma energy. As illustrated in Fig. 2(c), the stress field created by the He bubbles distributing in the fuzz layer will promote the upward migration of Mo atoms to the top of the structure, providing an advantageous driving force for the growth of the tendril fiber form of nanostructure known as fuzz.[31] Newly formed bubbles in the bottom layer of protrusions migrate and grow. Owing to the significant volume diffusion, the edge becomes sharper and the dips turn deeper in this process, which should be the root of increasing maximum height discrepancy of fuzzy surface. The swelling of He bubbles inside the nano-fuzz structure makes finer the tendril fiber at higher He energy, accelerating the fuzz development and the surface rougher tendency.

The morphological evolutions of nanostructured Mo surface under various He ion energy are systematically evaluated in terms of fuzz diameter, RMS roughness, and optical reflectivity, which are summarized in Fig. 3. To better quantitatively compare the fuzz difference to study the formation process of the fuzz, the obtained micrographs are equally divided into 25 parts in Image J software, 4 points of each fragment (totally 100 points) are selected to measure the diameters of fuzz filaments. Finally, the average fuzz diameter data are gained from the above-measured points via statistics with residual error bar added in Fig. 3(a) (displayed by redline). The diameter of the observed fiber-form filament is reduced from 58 nm to 39 nm with the enhancement of He ion energy as shown in Fig. 3(a). With the rising of plasma energy, the composite clusters of He and vacancy cross the energy barrier, and the mobility of He bubbles is improved, which makes He bubbles grow into a villus structure. Because of the discontinuity of the fuzz structure, the accumulation of heat makes the fuzzy surface rise, resulting in a temperature gradient and the stronger migration capability of the He-vacancy defect in the fuzz tip. Higher temperature accelerates the migration rate of nano-scale He bubbles in the fuzz structure, and it is conducive to the thinner fiber-form nanostructure growth observed at higher magnification in the inserted FE-SEM. This should be attributed to the growth of helium ion energy, playing a significant role in diffusion processes as in the present case.[32] The grain boundary diffusion takes place at lower temperatures whereas volume diffusion becomes significant only at higher temperatures. Since grain-boundary diffusion is orders of magnitude faster than volume diffusion, grain boundary is the pathway which the material transports through and so is the scenario in a low-porosity material. With the increase of heat load induced by growing helium ion energy, volume diffusion is activated significantly.[33] Thus the grain-boundary diffusion is dominated when helium ion energy is 50 eV, leading the crude protrusions to start to grow. And the development of the sharper and denser fiber-form filaments is the result of volume diffusion at higher helium ion energy. Owing to the the swelling of He bubbles inside the fuzz induced by the higher energy irradiation, the part of the longer fuzz structure grows in more random orientations. Therefore, it it is reasonable to observe in Fig. 3(a) that the measured RMS roughness of the fuzzy surface increases with the improvement of incident ion energy. The optical reflectivity is the ratio of radiant energy reflected by an object to the total radiant energy, which mainly

depends on the nature of the surface condition, especially the roughness. According to Bechmann's reflection probability model,[34] the reflectivity R is given by

$$R = R_0 \exp(-(4\pi r \cos\theta/\lambda)^2), \quad (1)$$

where R_0 is the reflectivity of an ideal smooth surface of the same material, r is the RMS roughness. This model does not consider the interaction between light and metal, so there will be a certain error with respect to the actual value, but the changing trend of reflectivity, caused by the change of roughness, is still of reference significance. Thus as shown in Fig. 3(b), the reflectivity of fuzzy surface is much lower than that of the pristine surface due to the increased RMS roughness. It is also reasonable to observe that the reflectivity of the Mo fuzzy surface induced by higher helium ion energy decreases due to the rougher nano-tendril fuzzy surface. The optical reflectivity of the surface decreases due to the presence of Mo fuzz nanostructures, and the degradation degree of optical property can be enhanced by increasing the fuzz density.[35]

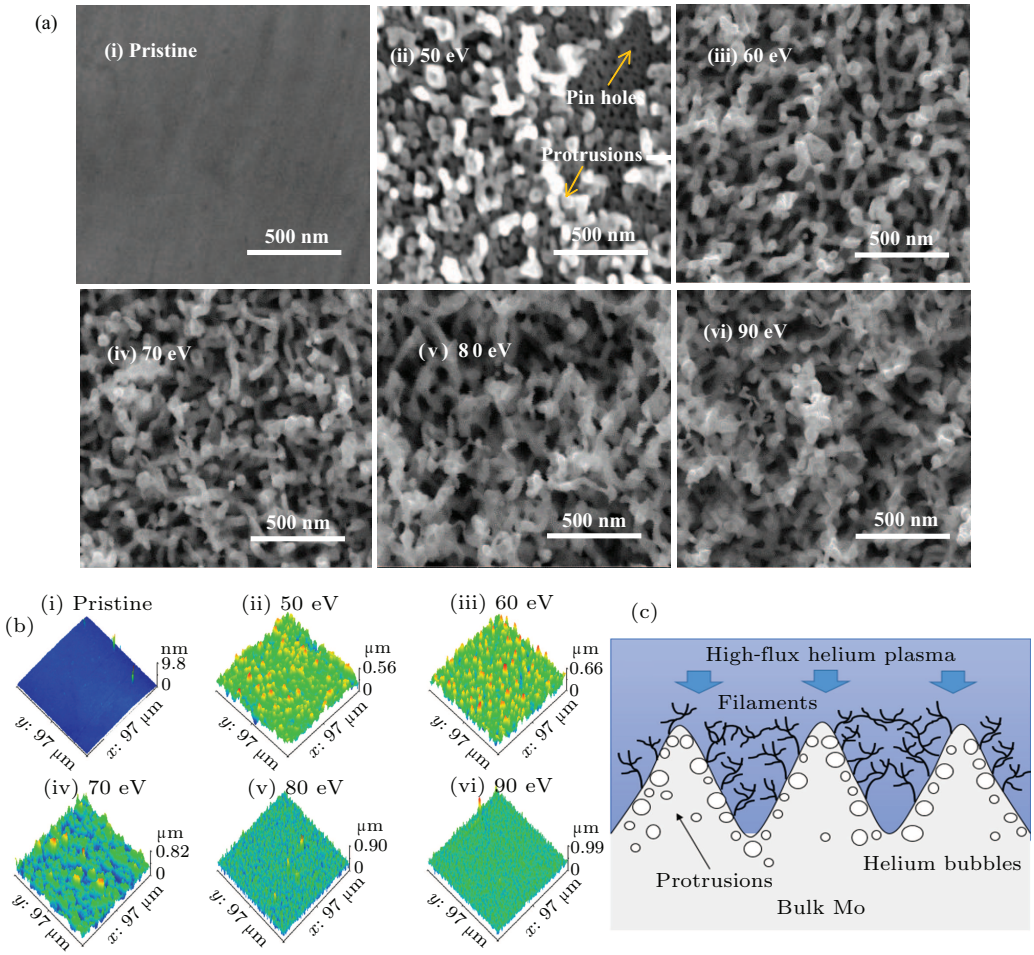


Fig. 2. (a) FE-SEM micrographs of Mo samples before and after being exposed to He plasma with high flux at ion energy in a range of 50 eV–90 eV, (b) 3D images of Mo samples before and after being exposed to He plasma with fixed high flux at ion energy in a range of 50 eV–90 eV, (c) schematic diagram for fuzz formation on Mo surfaces after being exposed to high flux helium plasma.

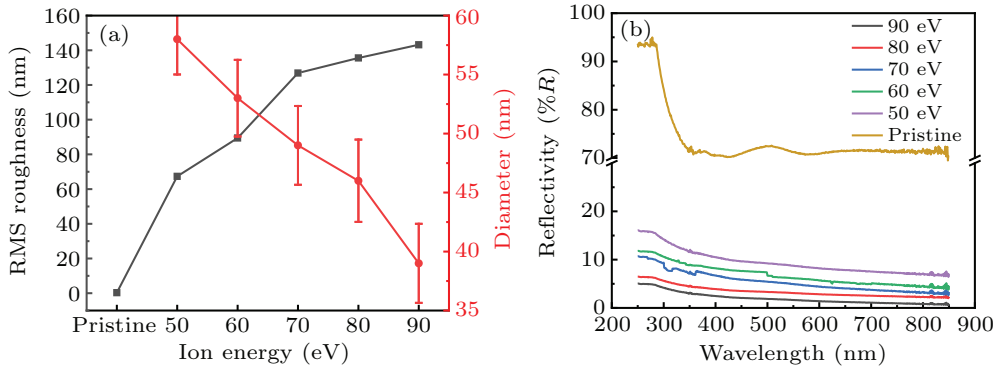


Fig. 3. Morphological parameters of nanostructured Mo surface varying with He ion energy, showing (a) RMS roughness of pristine and fuzzy molybdenum surfaces (left axis) and fiber-form filaments diameter (right axis) *versus* ion energy, and (b) reflectivity spectra for pristine and nanostructured Mo surfaces irradiated by He ions with different energies.

3.1.2. Crystal structure analysis from GIXRD pattern

Since the thickness of the fuzz layer is hundreds of nanometers, the grazing incident x-ray diffraction (GIXRD) is adopted to analyze the change of the fuzz layer. Scanning Mo surfaces is at an incidence angle of 1°, corresponding to an information depth of ~ 2 μm, so the degree of fuzzy surface evolution can be evaluated by GIXRD measurement results. It can be observed from the pattern that there exist four strong diffraction peaks of (110), (200), (211), and (220), for the crystal structure of the molybdenum sample can be indexed as a body-centered cubic (BCC) structure. It can be observed from Fig. 4(a) that the diffraction peak positions of pristine molybdenum shift toward the small angle side after being exposed to He plasma and the extent of each peak position shift is weakened by the rise of ion energy. Moreover, the diffraction peaks of the Mo surface after He plasma treatment becomes narrower with the increase of ion energy, indicating the grains growing in the fuzzy layer.

To better quantitatively investigate the crystal structure evolution, the structural parameters of Mo surfaces before and after being irradiated by He plasma are precisely calculated from the obtained GIXRD patterns.[36] For the lattice constant calculation, the Nelson–Riley function is used to achieve high-precision measurements of lattice parameter, which is given as follows:

$$a \sim \frac{\cos^2\theta}{\sin\theta} + \frac{\cos^2\theta}{\theta}, \tag{2}$$

where θ represents the peak position of diffraction peak, a is the lattice constant gained from four diffraction peaks according to Bragg law. It is plotted against the extrapolation function, and a straight line can be drawn through the points. The lattice constant corresponding to the value of 0 for the extrapolation function gives the true value of the lattice constant a. As for crystalline size, the peak broadening is the sum of widths due to small crystallite sizes and lattice strains. The $B\cos\theta$ is plotted against $\sin\theta$, where B is the full width at half maximum (FWHM) of the diffraction peak and θ is the peak position, B and θ are related by

$$B\cos\theta = \frac{k\lambda}{L} + \eta\sin\theta. \tag{3}$$

The crystallite size L can be calculated from the intercept by using the appropriate value of k (1.0) and λ (the wavelength of Cu K_α). As shown in Fig. 4(b), the lattice constant and crystalline size of the pristine sample, obtained from the measured peak positions of the crystal plane, are summarized and compared intuitively. On the one hand, the crystal lattice turns larger after having been treated by He plasma. This can be attributed to the fact that the He atoms diffuse into the near-surface layer of the substrate and occupy the interstitial sites in its sub-surface after having been irradiated by He plasma. As a result, the expanded crystal lattice is identified by the diffraction peak shifting to a small angle. On the other hand, the increasing surface temperature may be responsible for the growth of crystalline size. The grain boundary (GB) is one of the main nucleation regions of He atoms in metals since the He atoms exhibit a closed-shell electric structure and tend to sit at the sites with larger space, both substitutional and interstitial sites at GBs can provide larger space than those in the bulk, and thus He atoms prefer to stay in GBs.[37] The clear decoration of helium atoms at grain boundaries in bright-field TEM micrographs by El-Atwani *et al.*[38] has also supported the tendency of helium clusters to nucleate bubbles on grain boundaries. The tendency of He toms to accumulate at grain boundaries is a specific manifestation of the tendency of He atoms to accumulate at all types of free (excess) volume. Vacancies are also known to segregate at grain boundaries, creating the possibility of even more bound He atoms there.[39] The fewer the grain boundaries, the fewer the He atoms trapped in the near-surface region. Thus, the crystal lattice parameters of the fuzz layer generated at higher ion energy are smaller than those formed at lower ion energy.

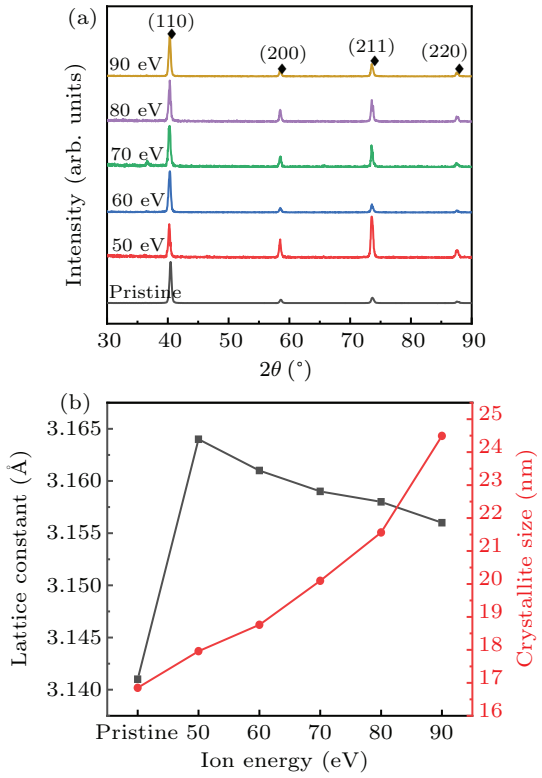


Fig. 4. (a) GIXRD patterns of Mo samples before and after being exposed to He plasma with high fluxes at various ion energies: 50 eV, 60 eV, 70 eV, 80 eV, and 90 eV. (b) Structural parameters obtained from x-ray measurements of fuzz molybdenum samples prepared by various ion energies.

3.2. Response of various Mo fuzz nanostructures to ELMs

Owing to the energy dispersion of helium ions interacting with the plasma-facing materials, it is necessary to investigate the influence of He ion energy on the response of fuzzy molybdenum surface to the density-fixed pulsed plasma. Nano-fuzz

molybdenum surfaces, produced by the steady He plasma with various ion energy in a range of 50 eV–90 eV, are subsequently exposed to pulsed plasma with the same power density. The selected power density of H-pulsed plasma (21 MW/m^2) is medium to avoid total fuzz removal, which is suitable to the studying of the etching process of fuzz structures induced by different ion energies. Like the Mo nano-fuzz formation study, the morphological evolution and the structural evolution of fuzzy surfaces after thermal shock induced by pulsed plasma are further investigated.

3.2.1. Morphological study of different Mo nanostructured fuzz melting damages

Melting can be clearly seen on the nano-structural fuzzy surface after a single H plasma shot. Figure 5 displays the surface morphologies of the regions irradiated by pulsed plasma, observed with an FE-SEM. The absence of fuzz on the surface, due to the molten droplet and dust release, can be observed in Fig. 5(b1). A large number of nano-pores can be seen to exist with a few nano-tendril fiber-form structures after being bombarded in Figs. 5(b2). As shown in Figs. 5(b3)–5(b5), the top layer of fuzz appears to begin melting after having been bombarded by pulsed plasma. Since He atoms occupy the interstitial sites in fuzzy surfaces, the thermal conductivity is greatly degraded by the accumulation of He clusters and the formation of He bubbles,[40] which should be the root of the fuzz melting aggravating with the helium ion energy decreasing.

More importantly, it is worth noting from the obtained micrographs that the extent of melting tends to be aggravated by the decrease of incident He ion energy. The response of the fuzzy surface to pulsed plasma loading is highly related to the condition of forming the fuzz, especially the incident ion energy. Combined with the results of the crystal structure analysis in Subsection 3.1.2, the crystallite size of the fuzzy surface decreases with the ion energy decreasing, meaning that the density of grain boundaries is higher. The He atoms tend to occupy the substitutional and interstitial sites in grain boundaries, which is evidenced by the larger lattice constant. The cluster of He atoms, which is a poor conductor of heat, leads the thermal resistance of the grain boundaries to increase. Under the same heat flux, a larger heat transfer temperature difference between grains needs to be maintained in the established heat transfer process. Therefore, the decrease of crystallite size inevitably weakens the heat transfer process of the fuzz layer and accelerates the degradation of thermal performance. During pulsed plasma bombardment, the fuzzy surface treated with the lower incident ion energy is more prone to the occurrence of severe melting damage and even molten droplet and dust release.

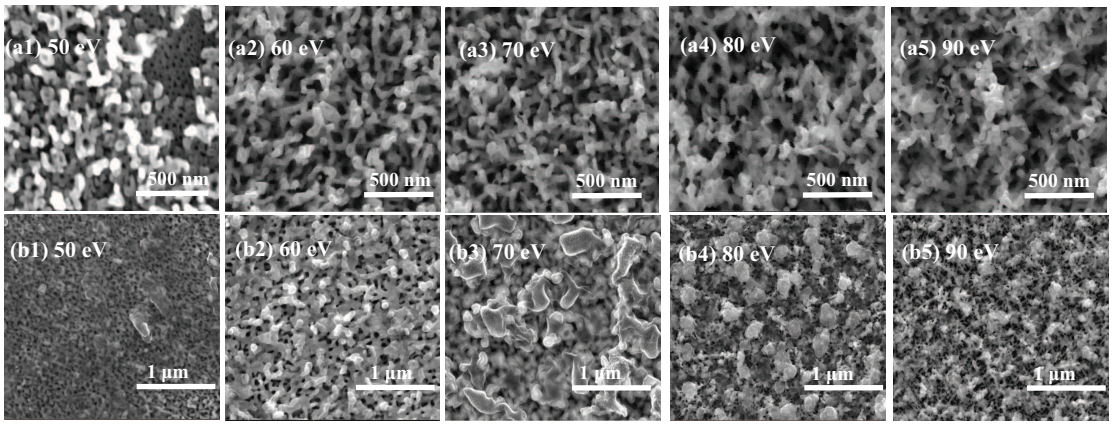


Fig. 5. Surface morphologies of Mo fuzzy surface (a1)–(a5) prepared by He plasma with various ion energies ranging from 50 eV to 90 eV and (b1)–(b5) subsequently bombarded by a single H-pulsed plasma.

The 3D images of bombarded fuzzy surfaces are obtained by an optical profiler (see supporting information in Fig. S3). The tips of the fuzzy layer are shrunk by melting damage and dust release, reducing the density of nano-tendril fiber form structure as depicted in Fig. 6(b). It is reasonable that the fuzzy surface is smoother after having been bombarded by pulsed plasma than those unirradiated ones. To further quantify the damage extent of various fuzz nanostructures under the same transient load conditions, the change of RMS roughness data after bombardment is shown in Fig. 6(c). From the figure it can be seen that the measured surface RMS roughness becomes smaller, suggesting that the fuzzy surfaces evolve more smoothly than prior-irradiated ones. Furthermore, the roughness of fuzzy surface prepared by lower-energy He ions changes more greatly, which is consistent with more severe damages evidenced by FE-SEM micrographs. Apart from optical profiler measurement, the reflectivity spectra are gained to compare the erosions of various fuzzes after pulsed load in another way. As shown in Fig. 6(d), the optical reflectivity of the fuzzy surface induced by lower-energy He ions recovers more than that induced by higher-energy ions after pulsed loading, meaning that the fuzzy surface by lower-energy ions tends to present more severe melting damage and turn smoother according to the introduced Bechmann's reflec-

tion probability model. The above discrepancy of the fuzz damage degree should be attributed to the various resistances to transient loads. Since the volume diffusion is increasingly activated by the improvement of ion energy, the fuzz filament turns thinner and the number and density of filaments on the top of the protrusion gradually increases during fuzz development. As illustrated in Fig. 6(a), the filaments on the adjacent protrusions are wound around each other and these entangled filaments will weaken the intensive transient thermal effect of plasma on its covered area. The denser structure is more conducive to the thermal response to the pulsed loads but the surface temperature is not easy to reach so fast that the severe molten dust release occurs. Thus the fuzzy surface prepared by higher-energy ions is more likely to survive after the same transient plasma treatment.

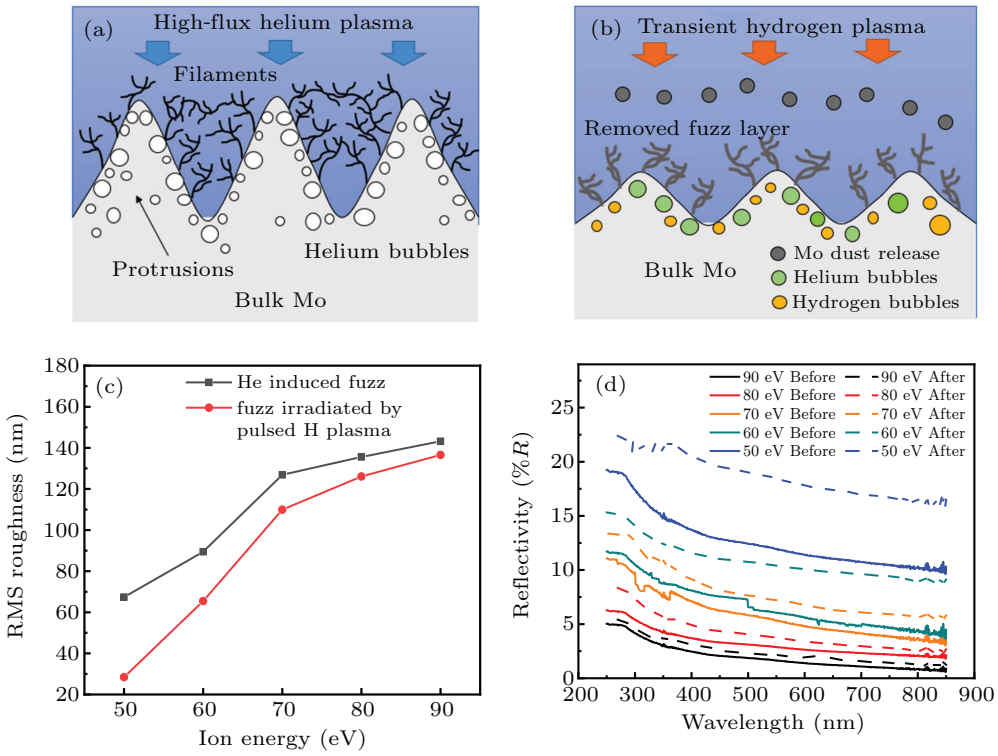


Fig. 6. (a) Schematic diagram for fuzz formation on Mo surfaces after being exposed to high flux helium plasma, (b) schematic diagram for fuzz removal by transient hydrogen plasma bombardment, (c) curves of RMS roughness *versus* ion energy for He-induced fuzz and fuzz irradiated by pulsed H plasma, (d) optical reflectivity spectra for various nanostructured surfaces exposed to pulsed loads.

3.2.2. Crystal structure evolution of various fuzz after transient irradiation

After the treatment of pulsed-H plasma, the evolution of phase structure at the fuzzy layer is analyzed by GIXRD. The measurement conditions are identical to those of the fuzz formation study. The measured patterns (see supporting information in Fig. S4) show that the peak positions have returned to the larger angle side, and the widths of the diffraction peaks also turn narrower than those of prior-irradiated fuzzy surfaces. To further compare the evolutions of structural parameters of various fuzzes after transient events, the lattice constants and crystallite sizes of fuzzy samples before and after being irradiated are calculated by the discussed methods and the results are shown in Fig. 7. From the figure it follows that with the increase of ion energy, the extent of damage to the crystal lattice constant declines and the crystalline size growth after the irradiation of the pulsed plasma gradually diminishes. When the lattice parameter declines, the high-flux helium irradiation produces the vacancy defects (V), which will interact with helium to form He–V clusters. According to the density functional theory, there exist more H trapping sites around He–V, and the binding energy of H ion with He–V is smaller than that of H ion with V.[41] As H ion capture center, the presence of He–V at the fuzz region makes the H ions diffuse to the surface more easily, which can inhibit the accumulation and deep diffusion of H ions.[42] Therefore, part of He ions, together with captured H ions by He–V, are thermally desorbed from the bombarded fuzzy surface, leading the lattice constant to shrink as indicated in Fig. 7(a). Besides the thermal desorption, the x-ray can penetrate deeper into the bulk Mo due to the removal of the fuzz layer, more structural information from unirradiated regions can be contained in the GIXRD patterns, reflecting on the weakened shift of peak position and decreased lattice constants. For the crystalline size growth, high temperature produces strong thermal effects during intensive pulsed irradiation, leading the molybdenum fuzzy surface to melt and the crystallite to continuously expand during the rapid cooling, which is evidenced by FE-SEM. Nevertheless, it has been universally received

that the tendency of He ions (as well as H ions) to accumulate at grain boundaries is a specific manifestation of isotope tendency to accumulate at all types of free (excess) volume where contained are the substitutional and interstitial sites for the He–V cluster and H ions trapping. Vacancies are also known to segregate at grain boundaries, creating the possibility of even more bound He ions and H ions there. Owing to the intensive thermal effect, the grown crystalline size can reduce the density of grain boundaries, which in turn provides less free space for isotope retention thereby reasonably explaining the reduction in lattice constants. Furthermore, it is worth noting that the fuzzy surfaces produced at lower-energy ions evolved more greatly in terms of lattice parameters and crystallite size. Various erosion degrees of the fuzz layer should be responsible for this phenomenon. According to the FE-SEM micrographs and optical reflectivity measurements, the Mo nano-fuzz turns denser with the increase of helium ion energy. Denser nano-fuzz structure with lower porosity is more beneficial to heat-shielding during transient thermal deposition. To some extent, the transient thermal response of fuzzy surfaces is more degraded by the decrease of He ion energy. Owing to less protection from dense filaments, the fuzzy surfaces induced by lower-energy helium ions are more directly faced with the transient plasma bombardment and more prone to the occurrence of serious molten fuzz removal, which is evidenced by morphological study. The more intensive thermal deposition can accelerate the growth of crystallite size as shown in Fig. 7(b). The effect is also reflected by the larger evolution of lattice constants. As the fuzz layers induced by lower-energy He ions are more greatly removed after transient events, on the one hand, x-ray can penetrate deeper beneath the fuzz nanostructure layer with more severe erosion, meaning that the penetration depth of the x-ray is more likely to exceed the irradiation range. The diffraction result includes both the ion irradiation region and the matrix. The structure of bulk material can affect the peak position of patterns, finally result in the more reduced lattice constants. On the other hand, H ions are more likely to be trapped by more He–V clusters and thermally desorbed by lower-density grain boundary resulting from the expanded crystalline grain during the intensive transient loading.[43]

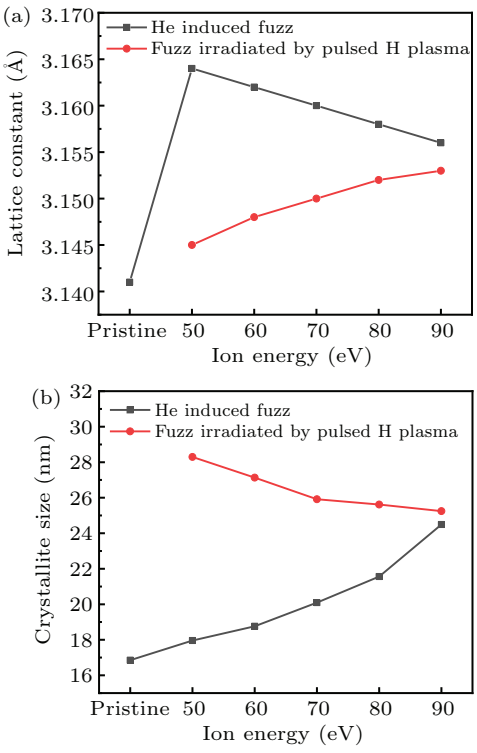


Fig. 7. Structural parameters obtained from x-ray measurements of different fuzz molybdenum samples and pulse-irradiated fuzzy samples; curves of (a) lattice constant and (b) crystallite size *versus* ion energy.

3.2.3. *Ex-situ* mass measurement of various damaged Mo nano-fuzz

To provide the quantitative reference for evaluating the various extents of damage to Mo nano-fuzzes, the total mass loss of fuzzy surfaces after pulsed-H plasma treatment is measured by electronic balance and it is plotted as a function of He ion energy as shown in Fig. 8, where can be seen the growth of fuzz mass loss with the decrease of He ion energy. The nanostructured fuzz induced by lower-energy He ions is more prone to the occurrence of dust release in the pulsed load process, which is consistent with the scenario in the above FE-SEM micrographs. Linear regression is fit to establish the quantitative relationship between the mass loss and He ion energy, and the following expression is obtained:

$$\Delta m_{\text{ion energy}} = 0.084E + 15.4, \tag{4}$$

where $\Delta m_{\text{ion energy}}$ represents the mass loss of fuzz and E denotes the He ion energy. The coefficient of determination for this regression is high, meaning that the data fit the regression line well. It can be seen from Fig. 8 that the fuzz nanostructures induced by lower-energy He ions are more easily removed from the molybdenum surfaces, which also supports the above morphological and structural studies. The fuzz induced by lower-energy He ions increases the potential of plasma contamination, which more attention should be paid to

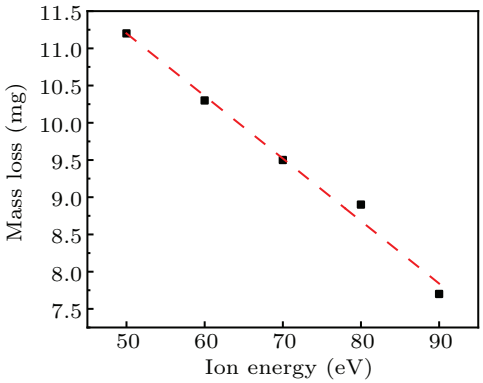


Fig. 8. Total mass loss of fuzzy Mo surface prepared by pulsed bombardment of different ion energies.

during transient events that have occurred during the H-mode in the tokamak.

3.3. Aggravated fuzz erosion by enhanced transient power density

The presence of such a fragile structure represents a serious threat to the sustainability of the confined plasma during transient events because the removal of even a small quantity of fuzzes can lead the plasma to immediately cool down. Thus it is indispensable to study the response of nanostructured fuzzes to various transient conditions. The fuzzy samples are treated firstly with He plasma with the same flux (5×10^{22} $m^{-2}\cdot s^{-1}$) and plasma energy (80 eV). For the transient power density-dependent study, the density and heat load of pulsed hydrogen plasma are both adjusted by the voltages applied to the power supply system. The density and heat load of pulsed plasma are set by adjusting the discharge voltage from 1000 V to 2000 V in gradient to simulate the growing severe operating environments. The degrees of fuzz damage caused by the irradiations of various pulsed plasmas can be characterized in terms of morphology and structure.

3.3.1. Recovery of Mo fuzzy surface morphologies by enhanced pulsed plasma

Figure 9 shows the FE-SEM images of pulsed-H plasma-treated Mo fuzz surfaces as a function of power density. It can be observed from the obtained micro-graphs that the melting loss of nano-fuzz is exacerbated with the improvement of discharge power. For the discharge power below 21 MW/m^2, the fuzz structure appearing on the top surface results from the process of melting and re-solidification, which is evidenced by the formation of coral-like protrusions. With the discharge power exceeding 21 MW/m^2, nano-tendrils (fuzz) begins to disappear, leading to smoother surfaces, and the widened cracks are observed in Fig. 9(h). Owing to the absence of nano-fuzz of the fuzzy surface resulting in the lack of heat shielding, bulk Mo material directly faces the transient plasma loads. The rapid change of surface temperature leads to strong thermal stress and severe brittle cracking. Under transient thermal shock, the surface temperature rises rapidly above the ductile–brittle transition temperature (DBTT) of molybdenum, and the grains are also expanded, resulting in strong compressive stress and plastic deformation. The irreversible expansion of the surface remains until the subsequent cooling process. During rapid cooling, the expansion of the grain volume shrinkage occurs immediately, resulting in huge tensile stress. With the enhancement of H-pulsed plasma, the increasing H flux makes more vacancies, resulting in the formation of H clusters. The growth of these clusters leads the hardness of the implanted specimen to increase.[44] Combined with considerable tensile stress caused by the intensive thermal load, the embrittled Mo material is easy to produce brittle cracking when the temperature drops below DBTT.

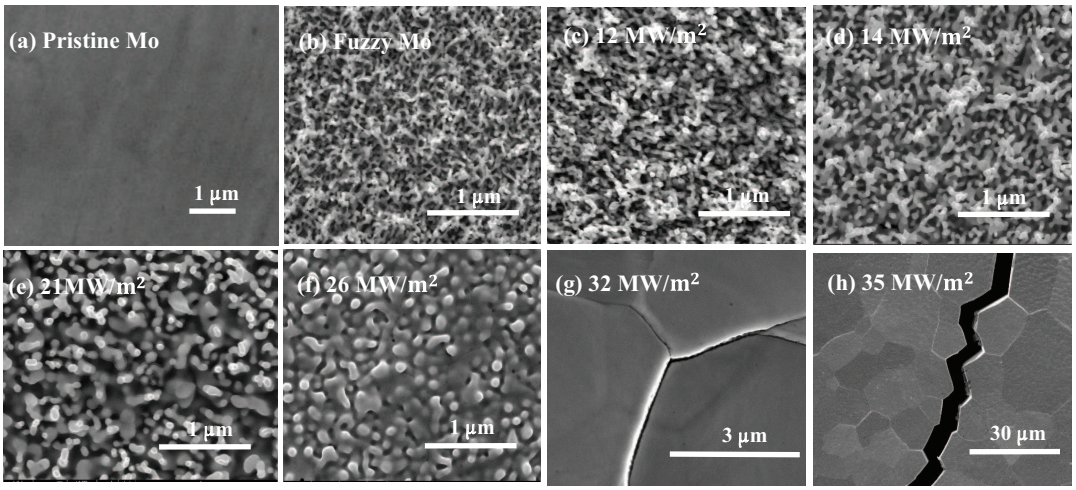


Fig. 9. Surface morphologies of (a) pristine and (b) fuzzy Mo samples prepared by He plasma with high flux, and (c)–(h) subsequently bombarded by single H-pulsed plasma with improved power.

As demonstrated in the 3D images obtained from the optical profiler (see supporting information in Fig. S5), the irradiated fuzzy surfaces become smoother due to the mass loss of nano-fuzz. The maximum height of irradiated fuzzy surfaces is slashed, corresponding to the shrinking of nano-structural fuzz as shown in the FE-SEM images. The fuzzy surface treated by higher power density becomes smoother and even closer to the condition of the pristine surface. According to the micrographs observed by FE-SEM and optical profiler, the fuzz nanostructure is intensively melted and even removed from the surface on the severe transient conditions. To further compare the damage degree of Mo fuzz by increasing pulsed load, the RMS roughness is summed up in Fig. 10(a). Moreover, the changing tendency of RMS roughness shows that the fuzzy surfaces evolve into smoother surfaces, which matches well with the morphological evolution as a function of pulsed

load intensity. The decline of the measured roughness results within the damaged area, together with the absence of fuzz evidenced by the topography by FE-SEM and the measured mass loss, indicates that the melting is induced by pulsed heat loading and more serious droplet release can be triggered off, finally resulting in flatter Mo surfaces with lower fuzz density.

Since the optical reflectivity of Mo nanostructured fuzzy surface offers an effective way to qualitatively characterize the evolution of fuzz in the transient loading process, reflectivity spectra are obtained for different pulsed load exposures as shown in Fig. 10(b). The optical reflectivity of the He-treated surface was nearly 1% due to the growth of nanostructured fuzz, which is much lower than that of the polished pristine surface. After the transient plasma bombardment, the observed recovery of surface optical reflectivity suggests the density of Mo fuzzes decreasing with the enhancement of pulsed load, which can be attributed to the deteriorated melting and more severe damage to nano-fuzzes. The fuzzy surfaces resulting from higher pulsed load treatment turns smoother according to the obtained RMS roughness. If there is no nanofilaments' block and the protrusions are wiped due to melting damage, the smoother metal surface can reflect the incident light in a more specific direction, thus obtaining higher optical reflectivity shown in the above reflectivity spectra.

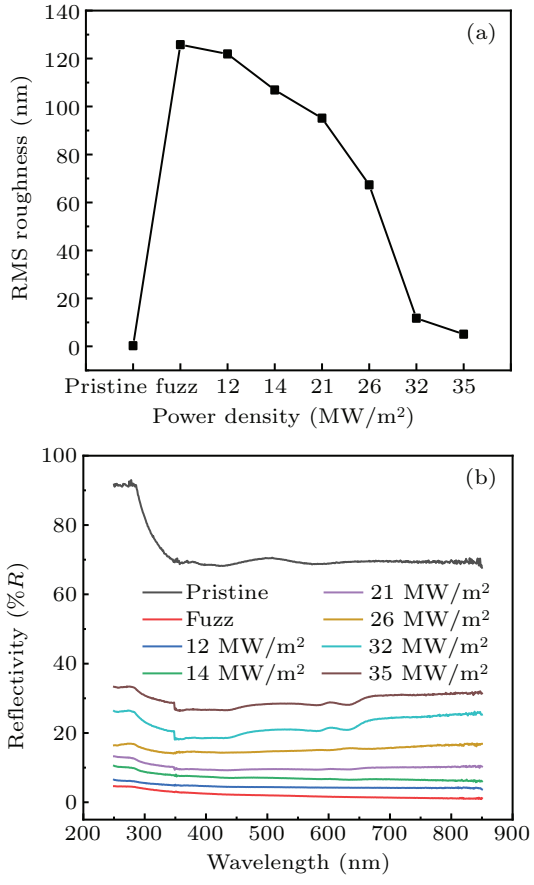


Fig. 10. (a) Power-density-dependent RMS roughness of fuzzy surfaces irradiated by enhanced pulsed loads, and (b) reflectivity spectra for pristine surface and fuzzy surfaces bombarded by enhanced pulsed loads.

3.3.2. Crystal structure evolution detected by GIXRD

The phase structures of fuzzy surfaces that have been bombarded by the enhanced transient plasma, are analyzed by grazing incidence x-ray diffraction. The incident angle is kept at 1° and the scanning range is between 30° and 90° to detect the information about the crystal structure of irradiated regions. It can be seen from the patterns (see supporting information in Fig. S6) that the phase structure of the body-centered cubic remains even after growing intensive pulsed irradiation. The diffraction peak position is observed to shift toward the high angle direction, indicating the lattice constant of molybdenum decreases after pulsed irradiation, caused by compressive stress accumulated in molybdenum. The narrower width of the diffraction peaks after pulsed treatment suggests that the molybdenum grains are coarsened. With the aggravation of fuzz structure damage, x-ray penetrated deeper beneath the fuzz layer and more structural information is obtained from the matrix. To quantify the damage degree of fuzzes in terms of phase structure, the lattice constants and grain sizes of the fuzzy surfaces before and after being irradiated, together with the pristine surface, are obtained from the GIXRD patterns. As shown in Fig. 11, the enlarged crystal lattice of the fuzzy surface shrinks gradually with the improvement of pulsed discharge power. On the one hand, with the enhancement of fuzz erosion, the matrix molybdenum material is more detected by x-ray and the calculated lattice constants are increasingly closer to the pristine ones. On the other hand, more He ions and captured H ions are thermally desorbed from the original fuzzy surface during enhanced transient loading due to serious damage to nano-fuzzes, thus less occupation by He and H leads to the smaller lattice constant.

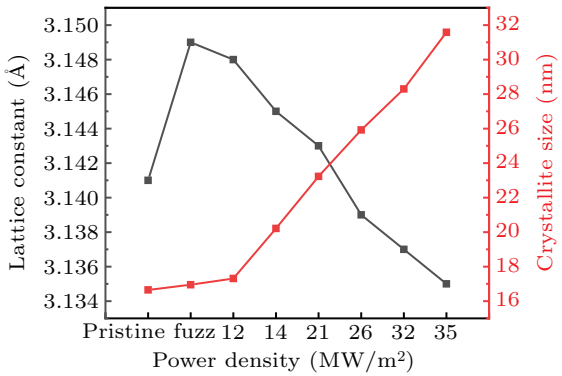


Fig. 11. Lattice constant and crystallite size of pristine Mo sample and fuzzy Mo sample subsequently bombarded by single pulsed-H plasma with improved power densities.

According to Fig. 11, the crystallite sizes of the irradiated fuzzy surfaces at higher discharge power are larger than those of pristine surface or irradiated surface by low-power pulsed plasma, indicating the growth of grain size during pulsed loading. The irreversible expansion of the surface remains until the subsequent cooling process. Thermal effects cause the

molybdenum surface to melt. Rapid cooling will accumulate a lot of stress in the metal. Once the surface faces even higher power-density transient plasma, when the surface stress reaches the critical limit, the growing crystallite is no longer resistant to plastic deformation,[45] which is evidenced by observed widening cracks left in FE-SEM after pulsed load treatment.

3.3.3. Mo fuzz etching and removal extent determined by mass loss measurement

The total mass losses of fuzzy surfaces after different pulsed load treatments are measured by electronic balance and they provide the quantitative reference for evaluating the extent of fuzz damage. The relationship between mass loss and energy density is shown in Fig. 12, and it can be observed from the figure that the mass loss of the removed fuzz and its growth rate increase with the augment of energy density of the pulsed plasma. To better quantify the relationship between the mass loss of fuzzy surface and the pulsed energy density, the exponential regression is used to fit the mass loss as a function of energy density. The $\Delta m_{\text{pulsed load}}$ represents the mass loss while Q denotes the energy density of pulsed plasma, and the exponential curve fit yields the following equation:

$$\Delta m_{\text{pulsed load}} = 0.50244\,\mathrm{e}^{0.2934(Q-17.0716)} + 4.7086. \quad (5)$$

The exponential regression line matches well with the mass loss data, evidenced by the high coefficient of determination (R^2) for this regression. The obtained equation can be used to predict the evolution of fuzz structure during the ELM. The increasing mass loss can be attributed to the more severe splashing of the melt layer by enhanced pulsed load, which greatly aggravates the plasma-enhanced surface etching and contamination. Prediction of potential contamination level is of great importance in evaluating the maximum lifetime of plasma-facing components in future fusion devices.

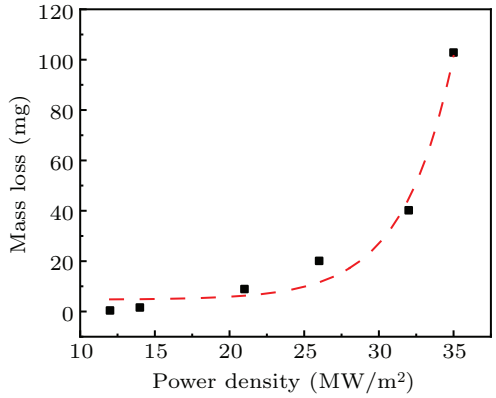


Fig. 12. Variation of total mass loss of fuzzy Mo surface after having been exposed to pulsed plasma with enhanced power density.

4. Conclusions

Molybdenum is currently considered as one of the most promising candidate materials for future plasma-facing components (PFC) due to its excellent thermal shock resistance and high melting point. The formation of nano tendril fiber structure (fuzz) on the molybdenum surface can be observed after having been treated by high-flux He plasma as demonstrated in the present work. During transient events that occur during plasma instabilities, large heat loads together with ion fluxes interact with the PFC, leading the fuzzes to be eroded and splashed. Concerns over the thermal shock performance of PFC necessitate the study of the evolution of fragile fuzz during pulsed plasma loading. Compact linear plasma device has great advantages in simulating steady and transient operating conditions and contributing to scientific studies of plasma and surface interaction issues. In this paper, the response of molybdenum nanostructured fuzzy surface to pulsed plasma bombardment by linear plasma device is explored. The conclusions can be drawn and summarized as follows.

(i) The damage to the fuzzy surface is aggravated with the increase of the pulsed-H plasma density. The melting of fuzz tips can be observed and evolved more severely with the increase of power density. When the power density of single pulsed-H plasma exceeds 21 MW/m^2, the nanostructured fuzzes are removed, and cracking happens due to transient heat load that can occur on the surface. The increased degradation of the fuzzy surface is also evidenced by the grown crystallite size and the recovery of the enlarged crystal lattice.

(ii) The degradation degree of fuzzy surfaces is enhanced by the decrease of the He ion energy of steady helium plasma. As the He ion energy decreases, the filaments of fuzz nanostructures are not dense enough to provide heat shielding during transient events. At the same time, more He ions tend to be trapped in the fuzzy layer, evidenced by more expanded crystal lattice which leads to lower thermal conductivity. The thermal separation between fuzzy layer and molybdenum bulk ensures thermodynamic non-equilibrium or a double layer in temperature. When the heat flux intensity is sufficiently high and its duration is short, the temperature of the fuzzy layer with worse thermal shock resistance is more prone to reaching melting point, resulting in more severe melting erosion and dust release. Correspondingly, more structural information from the matrix material affects the peak shift, finally leading the lattice constant to decrease. The expansion of crystalline is also accelerated during more intensive thermal shock, resulting in less H ions and He ions occupying the grain boundaries, which is the root of shrinking crystal lattice constants.

Acknowledgements

We are grateful to Hong-Bin Wang, Chi Yang, Zhi-Jun Wang for their help in the irradiation and characterization experiment.

Project supported by the Sichuan Provincial Science and Technology Program, China (Grant Nos. 2021YFSY0015

and 2021YJ0510), the China Postdoctoral Science Foundation (Grant No. 2019M663487), and the National Natural Science Foundation of China (Grant No. 11905151).

References

[1] Bolt H, Barabash V, Krauss W, Linke J, Neu R, Suzuki S, Yoshida N and Asdex Upgrade Team 2004 *J. Nucl. Mater.* **329–333** 66

[2] Brooks J N, El-Guebaly L, Hassanein A and Sizyuk T 2015 *Nucl. Fusion* **55** 043002

[3] Eren B, Marot L, Ryzhkov I V, Lindig S, Houben A, Wisse M, Skoryk O O, Oberkofler M, Voitsenya V S, Linsmeier C and Meyer E 2013 *Nucl. Fusion* **53** 113013

[4] Sharpe J P, Kolasinski R D, Shimada M, Calderoni P and Causey R A 2009 *J. Nucl. Mater.* **390–391** 709

[5] Wisse M, Eren B, Marot L, Steiner R and Meyer E 2012 *Rev. Sci. Instrum.* **83** 013509

[6] Temmerman G D, Bystrov K, Zielinski J J, Balden M, Arnas C and Marot L 2012 *J. Vac. Sci. Technol. A* **30** 041306

[7] Tanyeli R, Marot L, D Mathys, van de Sanden M and Temmerman G D 2015 *Sci. Rep.* **5** 9779

[8] Fiflis P, Connolly N and Ruzic D N 2016 *J. Nucl. Mater.* **482** 201

[9] Kajita S, Tokitani M, Saeki T, Ohno N and Yoshida N 2013 *J. Nucl. Mater.* **442** S515

[10] Yang Q, You Y W, Liu L, Ni W, Liu D, Liu C S, Benstetter G and Wang Y 2015 *Sci. Rep.* **5** 10959

[11] Sakamoto M, Miyazaki T, Higashizono Y, Ogawa K, Ozaki K, Ashikawa N, Tokitani M, Shoji T, Masuzaki S, Tokunaga K, Ohya K, Sagara A, Yoshida N and Sato K N 2009 *Phys. Scr.* **138** 014043

[12] Wright G M, Brunner D F, Baldwin M J, Doerner R P, Labombard B, Lipschultz B, Terry J L and Whyte D G 2012 *Nucl. Fusion* **52** 042003

[13] Wright G M, Brunner D, Baldwin M J, Bystrov K, Doerner R P, Labombard B, Lipschultz B, De Temmerman G, Terry J L, Whyte D G and Woller K B 2013 *J. Nucl. Mater.* **438** S84

[14] Baldwin M J and Doerner R P 2010 *J. Nucl. Mater.* **404** 165

[15] Sefta F, Juslin N and Wirth B D 2013 *J. Appl. Phys.* **114** 243518

[16] Kajita S, Yoshida N, Yoshihara R, Ohno N and Yamagiwa M 2011 *J. Nucl. Mater.* **418** 152

[17] Valles G, Martin-Bragado I, Nordlund K, Lasa A, Björkas C, Safi E, Perladom J M and Rivera A 2017 *J. Nucl. Mater.* **490** 108

[18] Takamura S 2014 *Plasma Fusion Res.* **9** 1405131

[19] Zohm H 1996 *Plasma Phys. Control. Fusion* **38** 105

[20] Voitsenya V S, Bardamid A F, Bondarenko V N, Jacob W and Vinnichenko M V 2001 *J. Nucl. Mater.* **290** 336

[21] Nishijima D, Kikuchi Y, Nakatsuka M, Baldwin M J, Doernei R P, Nagata M and Ueda Y 2011 *Fusion Sci. Technol.* **60** 1447

[22] Morgan T W, Zielinski J, Hensen B J, Xu H Y, Marot L and De Temmerman G 2013 *J. Nucl. Mater.* **438** S784

[23] Kajita S, Ohno N, Sakaguchi W and Takagi M 2009 *Plasma Fusion Res.* **4** 004

[24] Brooks J N, Allain J P, Doerner R P, Hassanein A, Nygren R, Rognlien T D and Whyte D G 2009 *Nucl. Fusion* **49** 035007

[25] Sinclair G, Tripathi J K, Diwakar P K and Hassanein A 2016 *Nucl. Fusion* **56** 036005

[26] Ye Z B, Ma X C, He P N, Wang Z J, Yang C, Chen B, Chen J, Wei J, Zhang K and Gou F J 2020 *Tungsten* **2** 94

[27] Zheng X J, Gou F J, Zhang Y P, Wang H X, Wallace A C, Wang H B, Huang Z H, Ji X Q, Ye Z B, Liang S Y, Zhang J Z, Wu N, Feng Y T and Deng B Q 2021 *Plasma Phys. Control. Fusion* **63** 035019

[28] Karl D Hammond 2017 *Mater. Res. Express* **4** 104002

[29] Cipiti B B and Kulcinski G L 2005 *J. Nucl. Mater.* **347** 298

[30] Zhou H B, Li Y H and Lu G H 2015 *Comput. Mater. Sci.* **112** 487

[31] Patino M I, Nishijima D, Tokitani M, Nagata D and Doerner R P 2021 *Nucl. Fusion* **61** 076001

[32] Tripathi J K, Novakowski T J, Joseph G, Linke J and Hassanein A 2015 *J. Nucl. Mater.* **464** 97

[33] Schwarz S M, Kempshall B W and Giannuzzi L A 2003 *Acta Mater.* **51** 2765

[34] Coates R 1988 *IEEE Transactions on.* **35** 522

[35] Tripathi J K, Novakowski T J and Hassanein A 2015 *Appl. Surf. Sci.* **353** 1070

[36] Suryanarayana C and Norton M G 1998 *Microsc. Microanal.* **4** 513

[37] Zhou H B, Liu Y L, Zhang Y, Jin S and Lu G H 2009 *Nucl. Instrum. Methods Phys. Res., Sect. B* **267** 3189

[38] El-Atwani O, HattarK, HinksJA, Greaves G, Harilal S S and HassaneinA 2015 *J. Nucl. Mater.* **458** 216

[39] Lejcek P and Hofmann S 1995 *Crit. Rev. Solid State Mater. Sci.* **20** 1

[40] Tokunaga K, Fujiwara T, Ezato K, Suzuki S, Akiba M and Yoshida N 2007 *J. Nucl. Mater.* **367** 812

[41] Becquart C S and Domain C 2009 *J. Nucl. Mater.* **386–388** 109

[42] Zhou H B, Momanyi N K, Li Y H, Jiang W and Li X C 2016 *RSC Adv.* **6** 103622

[43] Lee S C, Choi J H and Lee J G 2009 *J. Nucl. Mater.* **383** 244

[44] Zou H, Zhang L, Guan T, Zhang X N, Remnev G E, Pavlov S K, Wang Y N and Mei X 2020 *Surf. Coat. Technol.* **384** 125333

[45] Sinclair G, Tripathi J K, Diwakar P K and Hassanein A 2017 *Sci. Rep.* **7** 12273